Acoustic Oscillations in Solar and Stellar Flaring Loops

A. Kelly, V. M. Nakariakov and T. D. Arber

Space and Astrophysics Group, University of Warwick, Coventry, CV4 7AL, UK

E-mail: `kellya@astro.warwick.ac.uk`

Abstract
Observations of flaring loops in radio, visible and x-ray bands show quasi-periodic pulsations with periods from a few seconds to several minutes. Recent numerical studies have shown that some of these oscillations can be interpreted as standing slow magnetoacoustic waves. Energy deposition from the flare excites the second standing harmonic, with a period determined by the temperature and loop length. The excited longitudinal oscillations can be practically dissipationless and can, possibly, be considered MHD autowaves. Numerical simulations with a wide range of flare durations and choices of heat deposition location show that the second harmonic is a common feature of flaring loops.
Keywords: *Sun: corona, Sun: oscillations, MHD.*

1 Introduction

Observations of the solar corona provide us with many observations of oscillations and waves in a variety of wavelength bands and with a huge range of periodicities. We are interested in quasi-periodic pulsations (QPP) observed in coronal loops during solar flares. The flare causes a temporary increase in the intensity of the signal from the loop, followed by a cooling phase in which the intensity returns to its normal level. Quasi-periodic variations in intensity are seen during this cooling phase. These pulsations have periods from a few seconds up to thirty minutes. The two main mechanisms proposed for these oscillations are the sausage mode and slow magnetoacoustic mode. For the sausage mode there exists a cut-off which imposes a limit of around 20 s on the period. (Nakariakov et al., 2003) However, post-flare oscillations often show periods

much longer than this and thus the sausage mode cannot explain all observations. In this study, we develop further an alternative suggested in Nakariakov et al. (2004): flare-generated acoustic oscillations.

There are numerous observations of quasi-periodic compressible pulsations in coronal loops. For example, Wang et al. (2003) present a review of hot coronal loop oscillations as observed by SUMER with periods between 7 and 31 minutes. Harrison (1987) presents solar X-ray pulsations observed by the Hard X-Ray Imagining Spectrometer on the Solar Maximum Mission and reports a 24 minute periodicity. Similar oscillations but of shorter periodicity are presented by McKenzie et al. (1997) and Terekov et al. (2002). Wang and Xie (2000) observed flare associated pulsations in the microwave band with a period of about 50 s. Pulsations have been observed simultaneously in X-ray and microwave bands, for example by Fu et al. (1996) and Tian et al. (1999). Similar oscillations, have been observed in the stellar case such as the oscillation with a period of 220 s observed by Mathioudakis et al. (2003) on the star Peg II.

2   Numerical Model

We model coronal oscillations using a 1D radiative hydrodynamic code. The numerical code is a 1D version of the Lagrangian Re-map code (Arber et al., 2001). This code includes effects such as thermal conductivity, gravitational stratification and radiative losses. For the radiative loss function we use form given by Rosner et al. (1978) extended to a wider temperature range. (Peres et al., 1982; Priest, 1982) The simulation domain consists of a hot (initially 1 MK) coronal loop with a dense, cool (10^4 K) plasma region at each footpoint. This region mimics the chromosphere and acts as a source of plasma to fill the loop during the flare.

The flare is modelled by the application of a Gaussian heat pulse given by

$$E_H = E_0 \exp\left(-\frac{(s - s_0)^2}{2\sigma_s^2}\right)\left[1 + Q_P \exp\left(-\frac{(t - t_p)^2}{2\sigma_t^2}\right)\right], \tag{1}$$

where the energy deposition width is σ_s and its duration is σ_t. The flare amplitude is Q_p. This function includes time independent background heating which is applied in order to maintain the equilibrium. The magnitude of this background heating is given by E_0. For simplicity this background heating is applied at the same position as the flare. The default values for the various parameters are given in Tab. 1. In our analysis of the results times are quoted relative to the flare peak time, ie. $t - t_p$.

In the first phase of the simulation, the loop is allowed to settle into an equilibrium between radiative losses and the time independent heating function. Next the flare causes the temperature to rise and heat travels down the loop by thermal conductivity. This in turn causes evaporation of material from the model chromosphere to fill the loop. After the flare peak the loop cools and its temperature and density return to

Table 1: *Default simulation parameters.*

Parameter		Value
Loop Length	L	55 Mm
Initial Temperature	T	1 MK
Background Heating	E_0	0.004 erg cm^{-3} s^{-1}
Heating Width	σ_s	7 Mm
Flare Peak Time	t_p	7200 s
Flare Amplitude	Q_P	2×10^4
Flare Location	s_0	0 Mm (Apex)

their initial values. We study the oscillations which appear in the density, temperature and velocity profiles during this cooling process.

3 Data Analysis

We consider acoustic waves set up in a coronal loop due to an impulsive energy deposition. We observe these waves by analysing temperature, density and velocity time-series from the simulations. Temperature oscillations are of smaller amplitude than the velocity and density oscillations and therefore we don't examine them. The time series that we use are the variations at the apex. The structure of standing modes is such that odd numbered modes have a node in density at this point while odd numbered modes have a node in velocity. The standing wave has a frequency given by

$$f_n(T) = 152\frac{\sqrt{T}n}{L}.\tag{2}$$

The wave frequency changes with temperature and the temperature changes throughout the flare development. Thus, we can identify not the standing not just by the frequency, but by the appropriate modulation of the frequency with time. We use a Morelet wavelet transform (Torrence and Compo, 1998) to observe the distribution of wave power over both time and frequency.

Fig 1 shows time-series for the density at the loop apex and the average loop temperature for a typical flare. ($\sigma_t = 100$) As described in the previous section the density and temperature are seen to rise until the flare peak and then return slowly to their initial values. The density reaches its peak value after the temperature. Quasi-periodic variations can be clearly seen in the density, and less clearly in velocity.
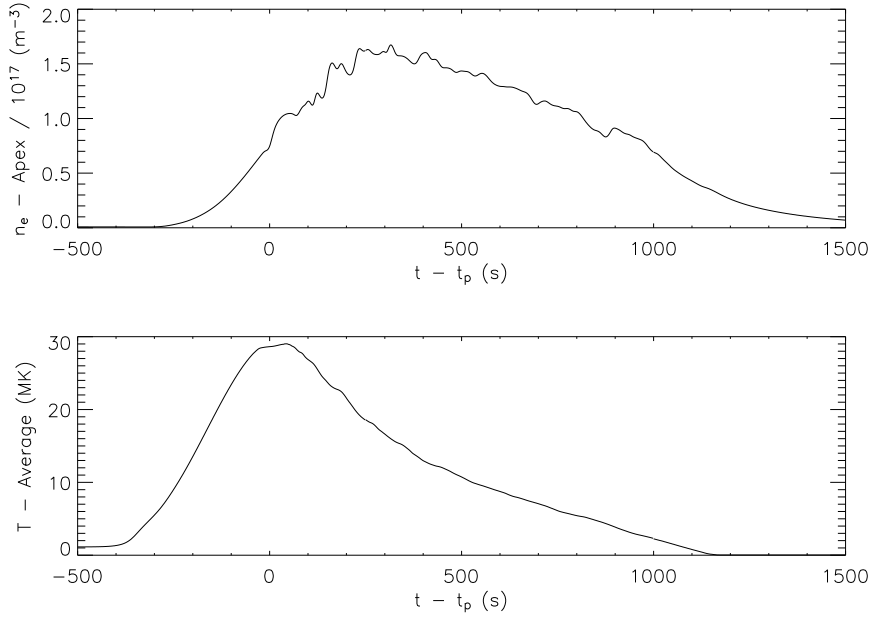
Figure 1: *Time evolution of the number density at the apex (upper panel) and average temperature (lower panel) for the $\sigma_t = 100$ s flare. ($Q_p = 2 \times 10^4$ and $s_0 = 0$)*

Before taking the wavelet transform we use a low pass filter to remove the long time scale variations from the signal. Fig 2 shows the filtered density from the 100 s flare and the wavelet the transform of this signal. This plot shows peaks in the wave power firstly around 200 seconds after the flare with a period of approximately 80 seconds and then later around 900 seconds after the flare with a period of approximately 180 seconds. The solid curved line across this plot shows the period of the harmonic. This oscillation with an amplitude of around 5–10% is the second harmonic standing mode acoustic wave.

As odd numbered modes have a node at the apex, it is unsurprising that the fundamental mode is not seen in these density plots. Fig 3 shows the velocity signal and its wavelet transform. There is no significant oscillation in the immediate aftermath of the flare with some oscillations appearing later. The wavelet transform shows that this later oscillation has power in the fundamental, second and fourth harmonics. We therefore conclude that the fundamental mode is not strongly excited by the energy
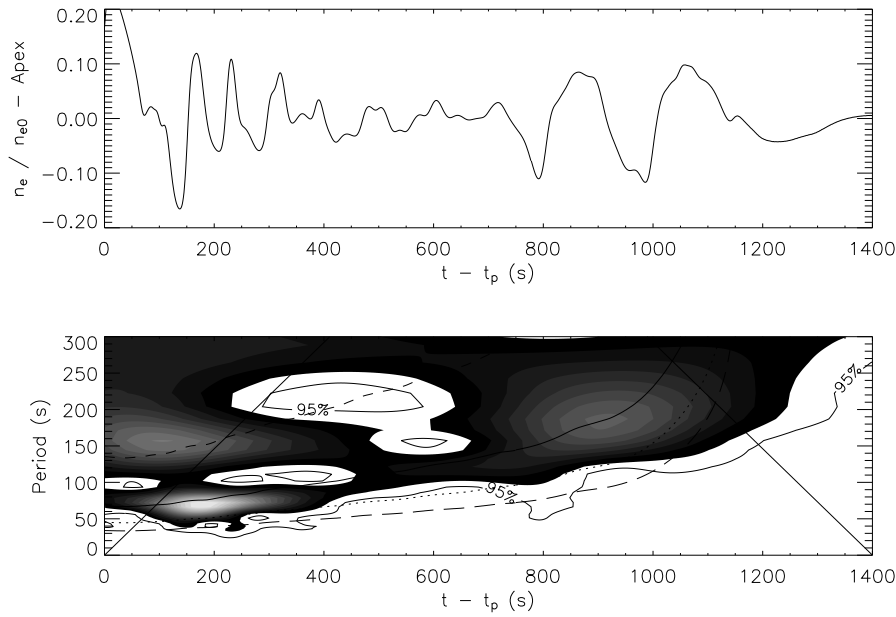
Figure 2: *The relative density oscillation n_e/n_{e0} at the apex for the 100 s flare (shown in Fig. 1) and a wavelet transform of the same signal. The curved lines across the wavelet transform show fundamental (upper dashed), second (solid), third (dotted) and forth (lower dashed) harmonic periods.*

deposition.

4   Discussion

The example shown in the previous section is a fairly typical simulation result. The second harmonic is seen to be the dominant excited mode for a wide range of flare parameters, while the fundamental mode is rarely seen. The second harmonic is a symmetric mode, and it would be natural to assume that the application of the flare at the apex leads to a symmetric oscillation. This, however, is not the case. The second harmonic continues to dominate, even when the flare energy is deposited asymmetrically at one footpoint. (Tsiklauri et al., 2004)

By examining the parameters of solar and stellar oscillations we can consider
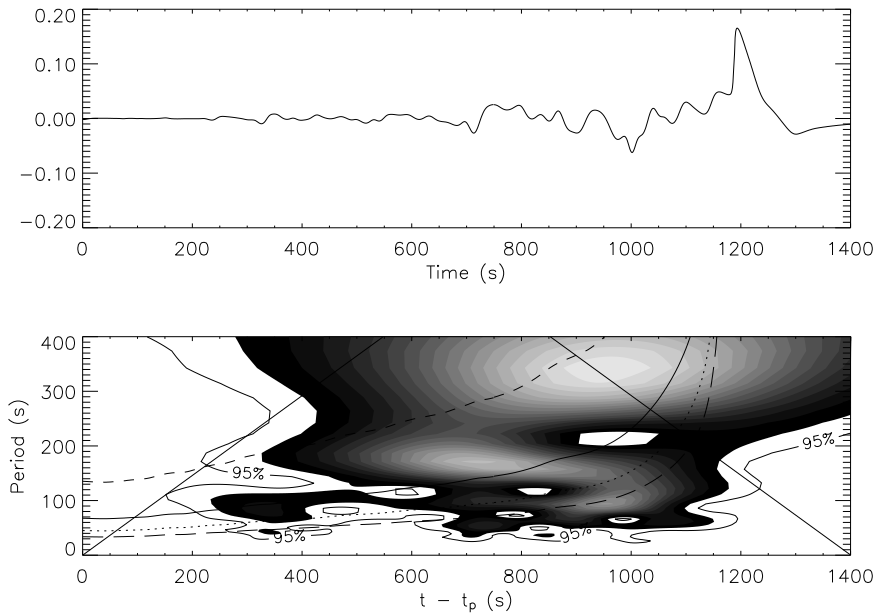
Figure 3: *The relative velocity oscillation V/C_S at the apex for the 100 s flare (shown in Fig. 1) and a wavelet transform of the same signal. The curved lines across the wavelet transform show fundamental (upper dashed), second (solid), third (dotted) and forth (lower dashed) harmonic periods.*

whether or not they are likely to be second harmonic standing acoustic waves as predicted by the simulations. Mathioudakis et al. (2003) studied white light oscillations during a flare on II-Peg and reported a period of 220 seconds. That paper gives estimates for the temperature and loop length of 200 MK and 500 Mm respectively. Using these values and Eq. 2, we can derive a value for the period of 233 seconds. This is consistent with the observed periodicity.

Considering solar observations Wang et al. (2003) examine a number of loop oscillations seen by SUMER. Many of these oscillations are not flare associated, but one example flare associated oscillation is that seen on the 29th of September 2000. An oscillation with a period of 28 minutes is observed in a loop with an estimated length of 515 Mm. This time, we can use Eq 2 to make a estimate of the temperature. This gives us a value of 4 MK. The observations are made using spectral lines at a

temperature of 6.4 MK.

The oscillations have two interesting properties. Firstly, they can persist for a number of oscillations with no significant damping, and sometimes even amplification. Secondly, they are often seen to disappear quite suddenly. The main dissipation mechanism for slow waves is well known to be thermal conductivity. From simple linear theory, the damping times for our example flare is 1.2 wave periods. Despite, this very strong damping several clear oscillations can be seen in Fig 2. As the oscillations appear despite the strong damping, then there must exist some instability which is amplifying the waves. One possible mechanism is the thermal instability. The simulation contains a heat loss function ($\mathcal{L}$) which gives the radiative losses from the plasma as a function of temperature. In the temperature regime at which oscillations occur $\frac{d\mathcal{L}}{dT} < 0$, meaning that cooler plasma loses energy more quickly. This instability can amplify waves. Waves may therefore exist in a balance between amplification due to thermal instability and high frequency dissipation. In order to test this hypothesis we run the flare simulations with radiative losses switched off. No oscillations are then seen in our example 100 s flare. If the waves are sustained by thermal instability then the waves would disappear suddenly when the temperature falls into the stable regime. This explains the sudden disappearance of the oscillations.

5 Conclusions

Observed quasi-periodic oscillations in coronal loops can be interpreted as standing magnetoacoustic waves. Hydrodynamic simulations of these waves show that energy deposition from a flare can excite standing modes and that the second harmonic is the most easily excited mode. This second harmonic seems to be the natural response of the loop to energy input and occurs for a wide range of energy deposition parameters such as position, duration and amplitude. The second harmonic is excited even for asymmetric energy deposition. The period of the oscillations can be calculated from the loop length and plasma temperature.

The acoustic waves interpretation is often excluded on the basis of strong thermal conductivity. Calculations based on the thermal conductivity suggest that the oscillations in our simulations should not occur. In the absence of thermal instability, these oscillations disappear and we therefore suggest that the waves exist as a result of competition between thermal over-stability and thermal dissipation.

References

Arber, T. D., Longbottom, A. W., Gerrard, C. L., Milne, A. M., 2001, J. Comput. Phys., 171 151.

Fu, Q.-J., Liu, Y.-Y., Li, C.-S., 1996, Chin. Astron. Astrophys, 20, 487.

Harrison, R. A., 1987, A&A, 182, 337.

Mathioudakis, M., Seiradakis, J. H., Williams, D. R., Avgoloupis, S., Bloomfield, D. S., McAteer, R. T. J., 2003, A&A, 403, 1101.

McKenzie, D. E., Mullan, D. J., 1997, Sol. Phys., 176, 127.

Nakariakov, V. M., Melnikov, V. F., Reznikova, V. E., 2003, A&A, 362, 1151.

Nakariakov, V. M., Tsiklauri, D., Kelly, A., Arber, T. D., Aschwanden, M. J., 2004, A&A, 414, L25.

Peres, G., Serio, S., Vaiana, G. S., Rosner, R., 1982, ApJ, 252, 791.

Priest, E. R., 1982, Solar Magnetohydrodynamics, Dordrecht,: D. Reidel Publ. Comp.

Rosner, R., Tucker, W. H., Vaiana, G. S., 1978, ApJ, 220, 643.

Terekov, O. V., Shevchenko, A. V., Kuz'min, A. G., et al., 2002, Astron. Lett., 28, 397.

Tian, D.-W., Gao, Z.-M., Fu, Q.-J., 1999, Chin. Astron. Astrophys., 23, 208.

Torrence, C., Compo, G. P., 1998, Bull. Amer. Meteor. Soc., 79, 61.

Tsiklauri, D., Nakariakov, V. M., Arber, T. D., Aschwanden, M. J., 2004, A&A, 422, 351.

Wang, M., Xie, R. X., 2000, Chin. Astron. Astrophys., 23, 208.

Wang, T. J., Solanki, S. K., Curdt, W., Innes, D. E., Dammasch, I. E., Kleim, B., 2003, A&A, 406, 1105.